IJIRSET
International Journal of Innovative Research in Science | Engineering | Technology

ISSN(O): 2319-8753
ISSN(P): 2347-6710

International Journal of Innovative Research in Science Engineering and Technology (IJIRSET)

(A Monthly, Peer Reviewed, Refereed, Scholarly Indexed, Open Access Journal)

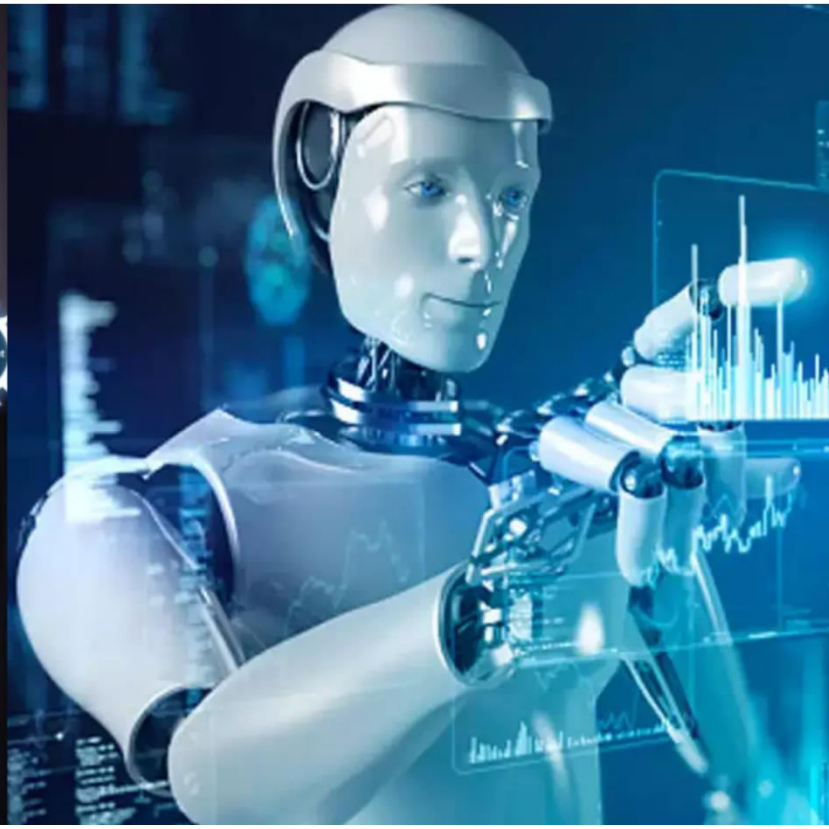

Impact Factor: 8.699

Volume 14, Issue 2, February 2025

International Journal of Innovative Research of Science, Engineering and Technology (IJIRSET)

Impact Factor 8.699

|www.ijirset.com |A Monthly, Peer Reviewed & Refereed Journal| e-ISSN: 2319-8753| p-ISSN: 2347-6710|

Volume 14, Issue 2, February 2025

|DOI: 10.15680/IJIRSET.2025.1402088|

Friction based Performance Study of Stabilizer Bar Bush Seal using Numerical Simulation

Ganesan Karthikeyan[1], Seok Sang Ho[2], Jo Jun Young[1], Jo Seung Hoon[3], Youn Geon-Ho[3], Han Se Heum[3]

Sr. Researcher, Adv. R&D Team, SECO AIA, 169, LS-ro, Gunpo-si, Gyeonggi-do, South Korea[1]

Principal Researcher, Adv. R&D Team, SECO AIA, 169, LS-ro, Gunpo-si, Gyeonggi-do, South Korea[2]

Researcher, Adv. R&D Team, SECO AIA, 169, LS-ro, Gunpo-si, Gyeonggi-do, South Korea[3]

ABSTRACT: This study conducts a detailed friction-based performance analysis of stabilizer bar bush seals through numerical simulations. Utilizing state-of-the-art Finite Element Analysis (FEA) tools, the research aims to evaluate how varying levels of friction coefficients impact the mechanical integrity and functionality of bush seals within automotive stabilizer bars. By systematically altering the friction coefficients from 0.1 to 0.5, the investigation assesses the resulting changes in reaction forces and stress distribution across the seal components.

The primary focus is on understanding how different friction settings influence the operational performance of the seals, particularly in terms of wear patterns, durability, and the ability to maintain effective load transmission between the stabilizer bar and its adjoining components. Key performance metrics such as seal deformation, stress resistance, and longevity under cyclic loading conditions are analyzed to provide insights into the optimal frictional properties required for maximizing seal efficiency.

The outcomes of this simulation study are expected to offer valuable guidelines for the design and material selection of bush seals, aiming to enhance the overall stability and noise, vibration, and harshness (NVH) characteristics of automotive suspension systems. Recommendations for future research will include exploring the impact of material heterogeneity and geometric modifications on the frictional behavior of stabilizer bar bush seals. This work sets a foundation for advancing the design standards of automotive bush seals by integrating friction considerations into the simulation protocols for component testing.

KEYWORDS: Seal, Stabilizer Bar Bush Seals, Finite Element Analysis (FEA), viscoelastic, Friction Coefficients

I. INTRODUCTION

The performance of automotive stabilizer bar bush seals is pivotal in maintaining the overall functionality and safety of vehicle suspension systems. These seals are integral components designed to protect stabilizer bars from external contaminants like dust and moisture while ensuring that the bar operates efficiently under various driving conditions. Their role extends to mitigating noise, vibration, and harshness (NVH), which are critical factors in enhancing passenger comfort and vehicle performance.

Role of Stabilizer Bar Bush Seals: Stabilizer bars, or anti-roll bars, are essential for reducing vehicle body roll during turns and sharp maneuvers. The bush seals act as cushions and provide necessary friction to maintain the position and effectiveness of the stabilizer bar. By preventing metal-on-metal contact, these seals significantly reduce the wear rate of the bar and suppress noise and vibrations that can occur due to the bar's movement. This dual functionality not only prolongs the life of suspension components but also improves the acoustic environment within the vehicle.

Challenges in Seal Performance: Despite their importance, the operational environment of bush seals is challenging. They are continuously exposed to road debris, chemicals, and extreme weather conditions, all of which can degrade the material properties of the seals over time. The rotational movement of the stabilizer bar during vehicle operation also subjects the seals to cyclic stress, potentially leading to material fatigue and failure if not designed and manufactured correctly.

International Journal of Innovative Research of Science, Engineering and Technology (IJIRSET)

Impact Factor 8.699

|www.ijirset.com |A Monthly, Peer Reviewed & Refereed Journal| e-ISSN: 2319-8753| p-ISSN: 2347-6710|

Volume 14, Issue 2, February 2025

|DOI: 10.15680/IJIRSET.2025.1402088|

Importance of Numerical Simulation: Numerical simulation, particularly through Finite Element Analysis (FEA), offers a sophisticated means of predicting and analyzing the performance of these seals without the need for extensive physical testing. FEA allows engineers to model the material behavior of the bush seals under various simulated conditions, assess stress and strain distributions, predict points of failure, and evaluate the impact of environmental factors on the material integrity. By understanding these aspects, improvements in material selection, geometric design, and overall seal performance can be systematically addressed.

Integrated Approaches in Seal Design: Recent advancements focus on integrating multiple functionalities into seal designs to address both sealing and NVH issues effectively. For instance, compound isolation designs, which combine materials with high and low damping properties, offer a balanced approach to manage NVH while maintaining good sealing performance [1]. These integrated approaches are becoming increasingly important as automotive systems become more complex and the demands for higher performance and lower emissions grow.

For research into bushing technology, developed a model addressing the lubrication of bearing bushes, challenging the adequacy of traditional liner models in representing hydrodynamic lubrication effectively [2]. Zhukov et al. explored the interplay between torsion and longitudinal shear in elastomeric bushings within the scope of nonlinear mechanics, suggesting that the torsional response could potentially influence the longitudinal shear stiffness [3].

In addressing challenges related to in-wheel motor systems, Tan et al. introduced a novel topology aimed at reducing the impacts of unsprung mass and deformation on the magnet gap, advocating for a design that optimally aligns the suspension with rubber bushings to maintain ride quality and comfort despite road surface irregularities [4].

Han et al. identified the design challenges associated with the viscoelastic hysteresis of rubber materials, which can lead to thermal failures in Positive Displacement Motor (PDM) stator bushings [5]. Conversely, Lindberg et al. successfully designed a rubber bushing model focused on noise and vibration reduction, achieving significant improvements in vibration mitigation [6].

Kaya utilized an integral algorithm for the design optimization of stabilizer bar bushings, yielding satisfactory outcomes [7]. Meanwhile, Puel et al. applied parameter identification techniques to nonlinear, time-dependent rubber bushing models, integrating these into multibody simulations for vehicle chassis analysis [8].

Zimmermann et al. employed finite element analysis to simulate the elastic modulus of natural rubber, providing critical engineering insights for bushing design [9]. Blom et al. introduced a dynamic torsional stiffness model for a magneto-sensitive circular annular rubber bushing, incorporating the effects of frequency, amplitude, and magnetic fields [10].

Tupholme designed a cylindrical rubber bushing, focusing on analyzing its radial stiffness [11], while Sedlaczek et al. developed advanced modular modeling and simulation approaches for automotive rubber bushings using dynamic mechanical models [12]. Lastly, Cerit et al. investigated the stress distribution and fatigue properties of rubber bushings, particularly noting how anti-roll bars in ground vehicles, which mitigate body roll, are prone to fatigue failure due to uneven vertical motion between wheels [13].

These studies collectively enhance our understanding of the dynamic interactions within bushing systems and their critical role in automotive design and performance.

II. STABILIZER BAR BUSH SEAL – OVERVIEW

Seals play an essential role in machinery, primarily designed to maintain lubricants within the system while keeping contaminants out. Their importance escalates in scenarios involving extreme environmental conditions or where high cleanliness standards are essential. By effectively integrating seals with the appropriate bearings and lubricants, it's possible to significantly reduce friction, enhance energy efficiency, and decrease the wear and tear on components.

International Journal of Innovative Research of Science, Engineering and Technology (IJIRSET)

Impact Factor 8.699

|www.ijirset.com |A Monthly, Peer Reviewed & Refereed Journal| e-ISSN: 2319-8753| p-ISSN: 2347-6710|

Volume 14, Issue 2, February 2025

|DOI: 10.15680/IJIRSET.2025.1402088|

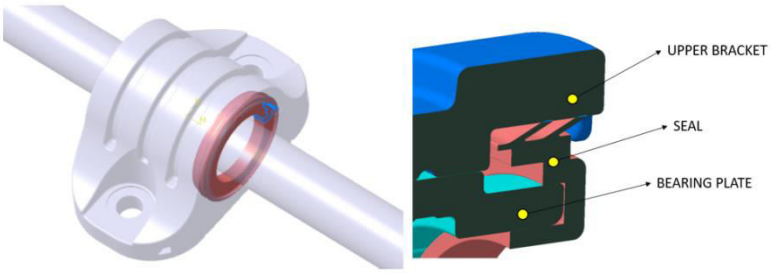

Figure 1. a. Seal in Stabilizer bar bush assembly, b. Section view of Stabilizer bar bush assembly, c. Nomenclature.

Currently, the automotive industry is undergoing a transformation like never before, driven by heightened environmental consciousness and increasingly rigorous emissions regulations. Seals are crafted for a multitude of components in both conventional and hybrid/electric vehicles, encompassing engines, drivelines, suspensions, and wheel-ends. Figure 1 illustrate the virtual Stabilizer bar bush assembly.

Radial shaft seals:
Radial shaft seals sit between rotating and stationary components, or two components in relative motion. They have two main parts. One is a cylindrical outer covering with an interference fit that seals statically against the housing bore. The second, a sealing lip, seals dynamically and statically against the shaft. Its sealing edge presses against the counterface surface of the shaft with a defined radial load [14]. Figure 2 illustrate the 3D CAD model of Seal and Figure 3 illustrate the manufactured part of seal and 3D CAD sectional view.

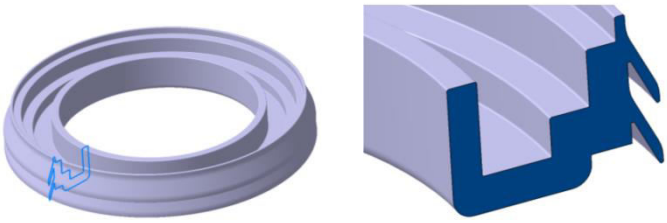

Figure 2. a. 3D CAD SEAL a. Full view, b. Section in detail view

Figure 3. a. Seal Production Part, b. Section view of 3D CAD SEAL

DIFFERENTIATION CRITERIA

- Sealing lip materials have high chemical/thermal resistance
- Superior pump rate
- Special coating compensates for housing bore surface imperfections

International Journal of Innovative Research of Science, Engineering and Technology (IJIRSET)

Impact Factor 8.699

|www.ijirset.com |A Monthly, Peer Reviewed & Refereed Journal| e-ISSN: 2319-8753| p-ISSN: 2347-6710|

Volume 14, Issue 2, February 2025

|DOI: 10.15680/IJIRSET.2025.1402088|

- Robust design
- Compliant with national and international standards

TYPICAL APPLICATIONS

- Gearboxes
- Hydraulic pumps
- Axles
- Power steering columns
- Speed reducers
- Transmissions
- Mount and bushes

III. DETERMINATION OF MATERIAL PARAMETERS

In this study, material parameters are are obtained in the formula (1) and derived using two primary approaches: numerical calculation and uniaxial tensile testing, with a specific emphasis on the latter. Uniaxial tensile testing is a fundamental component of accurately representing the hyperelastic material model for rubber in laboratory settings. To fully characterize the rubber's hyperelastic properties, three types of mechanical tests are typically required [24]: uniaxial tension (and compression), biaxial tension (and compression), and planar shear. Among these, uniaxial tension is notably the most straightforward and prevalently employed method for developing hyperelastic models in the analysis of rubber products. This paper specifically utilizes uniaxial tensile test data to enhance the precision of finite element analysis outcomes regarding the material properties under examination [25].

$$I_3 = (\lambda_1\lambda_2\lambda_3)^2 \quad (1)$$

Before conducting finite element analysis on rubber products, it is crucial to first understand the rubber's characteristics and constitutive equations, and then input the experimental parameters into the finite element software for material configuration. The properties of rubber are inherently complex, exhibiting nonlinear behavior that makes it challenging to define using simple parameters like those used for metals (such as elastic modulus and Poisson's ratio). Given its material and geometric properties, rubber is characterized as a non-linear, nearly incompressible material with a Poisson's ratio ranging from 0.45 to 0.5.

Although numerous researchers, both domestically and internationally, have proposed various test methods and constitutive equations for rubber, pinpointing an effective solution for these equations remains challenging. Consequently, there exists a variety of strain energy functions to describe the mechanical properties of rubber materials. Currently, the most commonly adopted constitutive equations include the Mooney-Rivlin model, introduced by Rivlin in 1976**,** and the Hookean-Neo model developed by Pence et al [15]**.** This paper will employ the Mooney-Rivlin model to explore these phenomena.

The expression of strain energy function of Mooney-Rivlin polynomial is [16]:

$$W = \sum_{n=1}^{N} C_{ij}\ (I_1 - 3)^i (I_2 - 3)^j + \frac{1}{2}\left(\sqrt{I_3} - 3\right)^2 \quad (2)$$

In the formula, W is the strain energy; ij C is the material parameter, i ≤1, j ≤1, i and j are positive integers; 1 I , 2 I and 3 I are one or two, three order Cauchy-Green strain tensor; K is the stretching length in three directions.

The relationship between 1 I , 2 I , 3 I and the three main stretching ratio 1λ , 2 λ , 3 λ of the hyperelastic material is [17-19]:

$$I_1 = \lambda_1^2 + \lambda_2^2 + \lambda_3^2 \quad (3)$$

$$I_2 = (\lambda_1\lambda_2)^2 + (\lambda_2\lambda_3)^2 + (\lambda_1\lambda_3)^2 \quad (4)$$

$$I_3 = (\lambda_1\lambda_2\lambda_3)^2 \quad (5)$$

International Journal of Innovative Research of Science, Engineering and Technology (IJIRSET)

Impact Factor 8.699

|www.ijirset.com |A Monthly, Peer Reviewed & Refereed Journal| e-ISSN: 2319-8753| p-ISSN: 2347-6710|

Volume 14, Issue 2, February 2025

|DOI: 10.15680/IJIRSET.2025.1402088|

Because the rubber is a hyperelastic material, approximate incompressible, assuming that the material is completely incompressible [20-23], that is, when 1 3 I = , the expression of strain energyfunction in (1) can be changed into the next [24]:

$$W = C_{10}(I_1 - 3) + C_{01}(I_2 - 3) \quad 6$$

where, C10 and C01 are non-zero material coefficients, which can be obtained by uniaxial tensile test. However, in the actual testing process, this model is difficult to capture the stiffness caused by the extension of the hyperelastic material caused by the increase, therefore the Bederman model has been further improved [25]:

$$W = C_{10}(I_1 - 3) + C_{20}(I_1 - 3)^2 + C_{30}(I_1 - 3)^3 + C_{01}(I_2 - 3) \quad 6A$$

In the formula, C10 , C20 , C30 and C01 are the material parameters, which can be obtained from uniaxial tensile test.

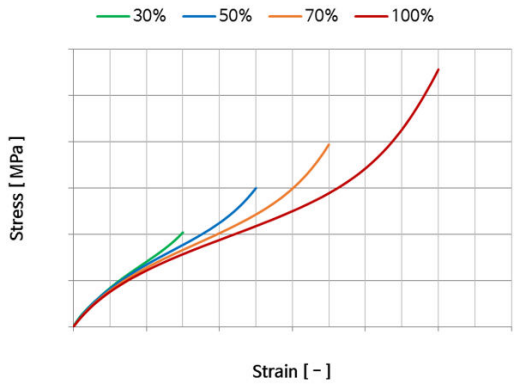

Figure 4. Seal Visco-elastic material Uniaxial Stress-Strain with different strain rate test data

For incompressible rubber materials, in the special case of uniaxial tension, the strain energy function corresponding to the engineering stress calculation formula is:

$$\hat{\sigma}_1 = \frac{\partial W}{\partial \lambda_1} = \frac{\partial W}{\partial I_1}\frac{\partial I_1}{\partial \lambda_1} + \frac{\partial W}{\partial I_2}\frac{\partial I_2}{\partial \lambda_1} + \frac{\partial W}{\partial I_3}\frac{\partial I_3}{\partial \lambda_1} \quad (7)$$

$$\hat{\sigma}_2 = \frac{\partial W}{\partial \lambda_2} = \frac{\partial W}{\partial I_1}\frac{\partial I_1}{\partial \lambda_2} + \frac{\partial W}{\partial I_2}\frac{\partial I_2}{\partial \lambda_2} + \frac{\partial W}{\partial I_3}\frac{\partial I_3}{\partial \lambda_2} \quad (8)$$

$$\hat{\sigma}_3 = \frac{\partial W}{\partial \lambda_3} = \frac{\partial W}{\partial I_1}\frac{\partial I_1}{\partial \lambda_3} + \frac{\partial W}{\partial I_2}\frac{\partial I_2}{\partial \lambda_3} + \frac{\partial W}{\partial I_3}\frac{\partial I_3}{\partial \lambda_3} \quad (9)$$

From the above three equations can be seen in the engineering stress and stretch ratio, the engineering error of stress and experimental values for [26-28]:

With all of the above formula with the experimental results, and ultimately obtained material parameters. And ABAQUS is to be solved, they are import the software to solve the problem [29].

$$S = \sum_{i=1}^{3} (\sigma_i - \sigma_i)^2 \quad 10$$

$$S = \partial s / \partial C_{ij} = 0 \quad 11$$

International Journal of Innovative Research of Science, Engineering and Technology (IJIRSET)

Impact Factor 8.699

|www.ijirset.com |A Monthly, Peer Reviewed & Refereed Journal| e-ISSN: 2319-8753| p-ISSN: 2347-6710|

Volume 14, Issue 2, February 2025

|DOI: 10.15680/IJIRSET.2025.1402088|

IV. SEAL - NUMERICAL SIMULATION

Overview: The "SEAL CAE Process" outlines a robust framework for automating and optimizing simulation processes in engineering, particularly focusing on sealing applications within automotive and aerospace industries. The process leverages various scripting and automation techniques to streamline the creation of simulation models, execution of analysis variants, and management of output data.

1. Simulation Setup: The initial step involves setting up the base simulation models in CAE software like Abaqus. This includes defining geometric parameters, material properties, and boundary conditions relevant to sealing applications. Variants of these base models are generated to explore different design scenarios and operational conditions.

2. Generating Variants: Using Python scripting within Abaqus, multiple variants of the base model are created to test different combinations of parameters such as material types and physical properties. Each variant is automatically adjusted to reflect specific test conditions or design changes, ensuring a thorough exploration of the design space.

- **Material Variants:** Different materials are tested to understand their impact on the performance and durability of the seal.
- **Load and Boundary Conditions:** Variations in operational conditions are simulated by altering load and boundary conditions across the models.
- **Solution parameters setup:**

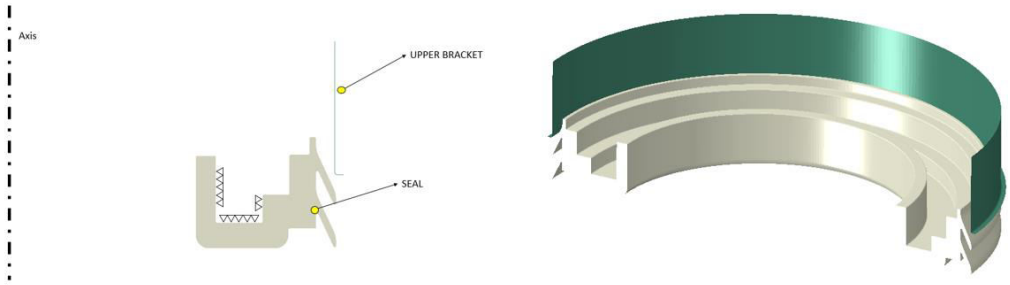

Figure 5. a. Axisymmetric model, b. Half model

The analysis in this study was conducted using Abaqus, a robust commercial software known for its capabilities in nonlinear simulation. The specific approach taken involved utilizing a 2D axisymmetric model, which is ideal for examining symmetrical components such as the upper bracket assembly integrated with a seal. This modeling choice effectively simplifies the computational process while still providing accurate insights into the assembly's behavior under simulated conditions.

To evaluate the performance characteristics of the seal in the bracket assembly, friction was chosen as the primary factor. This study systematically varied the friction coefficients to observe their impact on the assembly's performance, setting the coefficients at 0.1, 0.2, 0.3, 0.4, and 0.5. These values allowed for a comprehensive analysis of how friction influences the operational efficiency and wear characteristics of the seal within the assembly.

Additionally, the contact area between the bearing plate and the seal was fixed to eliminate any variables that could affect the accuracy of the friction impact assessment. This constant ensures that changes in the performance characteristics observed in the model are due solely to the varying levels of friction, providing a clear view of how friction affects the seal's functionality and durability.

International Journal of Innovative Research of Science, Engineering and Technology (IJIRSET)

Impact Factor 8.699

|www.ijirset.com |A Monthly, Peer Reviewed & Refereed Journal| e-ISSN: 2319-8753| p-ISSN: 2347-6710|

Volume 14, Issue 2, February 2025

|DOI: 10.15680/IJIRSET.2025.1402088|

This methodological approach not only enhances the reliability of the performance evaluation but also aids in the identification of the optimal friction coefficient that balances efficiency and wear resistance in the seal assembly. Such detailed analysis is crucial for designing components that can withstand real-world operational conditions while maintaining high performance and longevity.

The boundary conditions to simulate the deformation of the weather-strip seal assembled on the door surfaces which have bent or twisted profiles were set as follows:

In the simulation setup described:

1. Fixed Bearing Plate: The location of the bearing plate is secured with all degrees of freedom (DOF) being restricted. This setup, as illustrated in Figure 5a, ensures that the bearing plate serves as a stable reference point or base within the model. By fixing all DOFs, any movement, rotation, or other forms of displacement are prevented, allowing the simulation to accurately measure the effects of other moving parts without interference from the base.

2. Upper Bracket Movement: The upper bracket is specifically manipulated to move downward by 7mm to maintain the desired assembly position. This movement is critical to simulate real-world operational conditions where the bracket may be subjected to forces that require it to shift within certain limits. The 7mm displacement ensures that the assembly remains in an appropriate position to evaluate performance under a controlled yet realistic scenario.

By elaborating on these points, it becomes clear that the model setup is carefully designed to mimic practical conditions while providing a stable framework to evaluate the interactions and performance of the components within the assembly. Such precision in setting the parameters of the model helps in obtaining reliable and applicable results from the simulation.

V. RESULTS OF THE NUMERICAL SIMULATION OF SEAL

Figure 6 depicts the initial stages of the simulation process, showcasing the position of the upper bracket relative to the seal lips, identified as lip-1 and lip-2. This setup provides a clear view of the bracket's approach toward each lip, setting the stage for further interaction analysis during the simulation.

Figure 7 presents a 3D sectional view that illustrates both the stress distribution and displacement contours within the seal after assembly with the upper bracket. This visualization is crucial for assessing the mechanical stress responses and deformation patterns across the seal, providing insights into the structural integrity and potential areas of stress concentration under applied loads.

In Figure 8, a detailed view of the contact status on the seal's lips, as they interface with the upper bracket, is provided. The contact status contour detailed in this figure explains how the seal lips engage with the upper bracket, highlighting the nodal displacement interactions. This aspect of the simulation focuses on the precise points where the seal and bracket meet, offering a granular look at how the seal conforms to the bracket's surface and how this contact influences the seal's performance. This detailed mapping of contact points is essential for understanding the seal's effectiveness in maintaining a tight closure and identifying potential points of failure due to improper contact or excessive stress

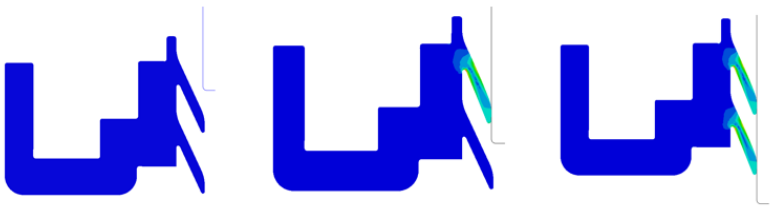

Figure 6. a. Before assembly, b. assemble until First lip, c. Fully assembled condition

International Journal of Innovative Research of Science, Engineering and Technology (IJIRSET)

Impact Factor 8.699

|www.ijirset.com |A Monthly, Peer Reviewed & Refereed Journal| e-ISSN: 2319-8753| p-ISSN: 2347-6710|

Volume 14, Issue 2, February 2025

|DOI: 10.15680/IJIRSET.2025.1402088|

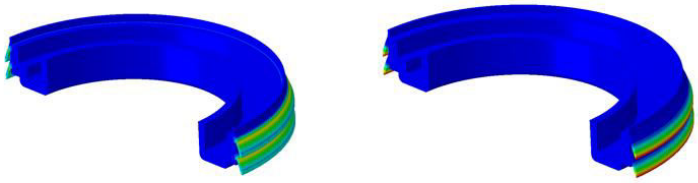

Figure 7. a. Stress plot, b. Displacement plot

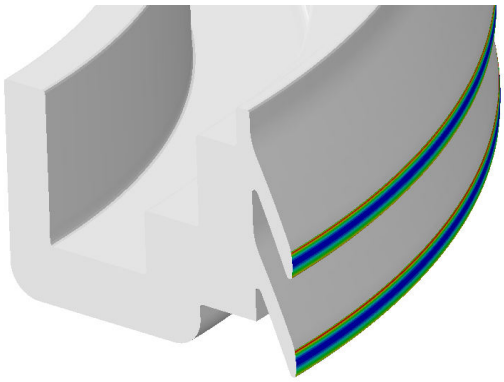

Figure 8. Contact status of Lip

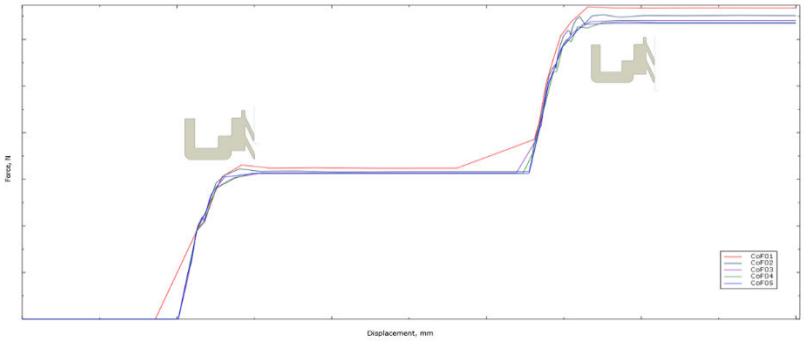

Figure 9. Reaction force on Lip for graph

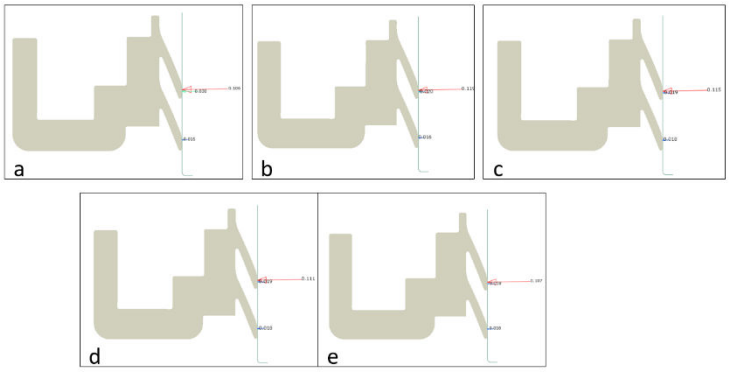

Figure 10. Normal force vector plot a.CoF 0.1, b.CoF 0.2, c.CoF 0.3, d.CoF 0.4, e.CoF 0.5,

International Journal of Innovative Research of Science, Engineering and Technology (IJIRSET)

Impact Factor 8.699

|www.ijirset.com |A Monthly, Peer Reviewed & Refereed Journal| e-ISSN: 2319-8753| p-ISSN: 2347-6710|

Volume 14, Issue 2, February 2025

|DOI: 10.15680/IJIRSET.2025.1402088|

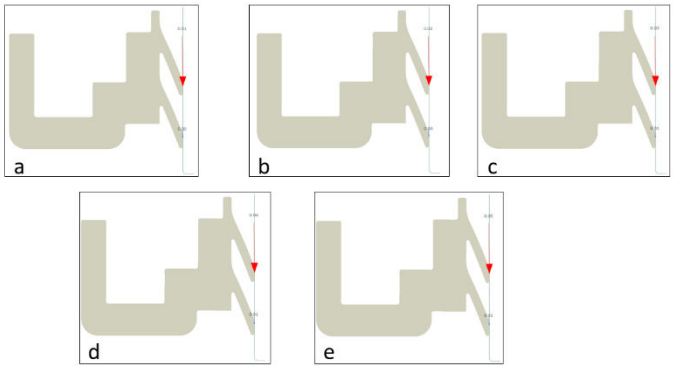

Figure 11. Shear reaction force vector plot a.CoF 0.1, b.CoF 0.2, c.CoF 0.3, d.CoF 0.4, e.CoF 0.5,

Figure 9 provides an analysis of the reaction forces exerted by the upper bracket, illustrating how these forces increase across different coefficients of friction—0.1, 0.2, 0.3, 0.4 and 0.5. This increase is notably observed at both lip-1 and lip-2 of the seal, highlighting the impact of friction on the force dynamics between the seal and the bracket. Additionally, the figure illustrates the variance in reaction forces at different friction levels, providing a clear distinction in how friction affects the mechanical interaction at each lip.

Figures 10 and 11 delve deeper into the specific types of forces—normal and shear—acting on the seal when assembled with the upper bracket under the same range of friction coefficients. These figures elucidate that lip-1 (the upper lip) typically experiences higher reaction forces when engaged with the upper bracket, while lip-2 (the lower lip) exhibits comparatively lower reaction forces. This differential in force distribution underscores the distinct roles that each lip plays in the seal's functionality.

The dynamics of normal contact forces are particularly intriguing:

- On lip-1, there is a gradual increase in normal forces from a friction coefficient of 0.1 to 0.2.
- This is followed by a decrease from coefficients 0.3 to 0.5, indicating a complex interaction between surface friction and the material response.
- Conversely, on lip-2, the normal forces decrease between friction coefficients of 0.1 and 0.2, but then increase from 0.3 to 0.5.
- These observations suggest that the contact mechanics between the seal lips and the upper bracket are significantly influenced by the level of friction, affecting how firmly each lip can maintain contact under varying conditions. Despite these fluctuations, the seal maintains robust contact with the upper bracket across all tested friction conditions, ensuring effective sealing and mechanical stability.

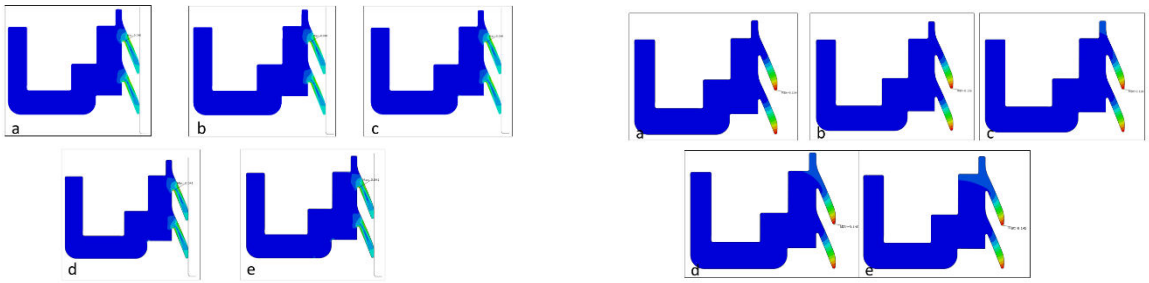

Figure 12. A. Stress plot B. Displacement plot (a.CoF 0.1, b.CoF 0.2, c.CoF 0.3, d.CoF 0.4, e.CoF 0.5)

International Journal of Innovative Research of Science, Engineering and Technology (IJIRSET)

Impact Factor 8.699

|www.ijirset.com |A Monthly, Peer Reviewed & Refereed Journal| e-ISSN: 2319-8753| p-ISSN: 2347-6710|

Volume 14, Issue 2, February 2025

|DOI: 10.15680/IJIRSET.2025.1402088|

VI. SUMMARY, CONCLUSION & FURTHER PROCEEDINGS

This study thoroughly analyzed the effects of varying coefficients of friction on the reaction forces exerted by the upper bracket against the seal in an automotive setting, using a numerical simulation approach with Abaqus. The findings indicated significant variations in reaction forces at different friction levels, particularly between the two lips of the seal—lip-1 and lip-2. Lip-1 consistently experienced higher reaction forces, suggesting it plays a more critical role in seal integrity and performance. The investigation of normal and shear forces further highlighted the complex interplay between friction levels and force response, suggesting a nuanced understanding of seal behavior under different operational conditions.

To build on the findings from this study, several avenues for further research are proposed:

Outer Diameter Variants of Upper Bracket: Exploring how changes in the outer diameter of the upper bracket influence the stress distribution and overall performance of the seal could provide deeper insights into optimal bracket sizing and its impact on durability and efficiency.

Material Variants: Investigating different rubber material compositions for the seal could uncover better performance characteristics such as durability, flexibility, and friction behavior. Materials with varying degrees of elasticity, thermal stability, and wear resistance could be tested to find the best match for specific automotive applications.

REFERENCES

[1] Lu, Y. C. (2007). Effects of seal viscoelastic properties on engine exterior cover noise and vibration. SAE Technical Papers on CD-ROM/SAE Technical Paper Series. https://doi.org/10.4271/2007-01-2285
[2] W. Litwin, Properties comparison of rubber and three layer PTFE-NBR-bronze water lubricated bearings with lubricating grooves along entire bush circumference based on experimental tests, Tribol. Int. 90 (2015) 404-411.
[3] B. A. Zhukov, Nonlinear interaction of finite longitudinal shear with finite torsion of a rubber-like bushing, Mech. Solids 50(3) (2015) 337-344.
[4] D. Tan, C. Lu, C. B. Ren, Optimal matching between the suspension and the rubber bushing of the in-wheel motor system, P. I. Mech. Eng. D-J. Aut. 229(6) (2015) 758-769.
[5] C. J. Han, J. Zhang, Z. Liang, Thermal failure of rubber bushing of a Positive Displacement Motor: A study based on thermo-mechanical coupling, Appl. Therm. Eng. 67(1-2) (2014) 489-493.
[6] E. Lindberg, M. Ostberg, N. E. Horlin, et al., A vibro-acoustic reduced order model using undeformed coupling interface substructuring - application to rubber bushing isolation in vehicle suspension systems, Appl. Acoust. 78 (2014) 43-50.
[7] N. Kaya, Shape optimization of rubber bushing using differential evolution algorithm, Sci.World J. (2014) 379196.
[8] G. Puel, B. Bourgeteau, D. Aubry, Parameter identification of nonlinear time-dependent rubber bushings models towards their integration in multibody simulations of a vehicle chassis, Mech. Syst. Signal Pr. 36(2) (2013) 354-369.
[9] J. Zimmermann, M. Stommel, The mechanical behaviour of rubber under hydrostatic compression and the effect on the results of finite element analyses, Arch. Appl. Mech. 83(2) (2013) 293-302.
[10] P. Blom, L. Kari, The frequency, amplitude and magnetic field dependent torsional stiffness of a magneto-sensitive rubber bushing, Int. J. Mech. Sci. 60(1) (2012) 54-58.
[11] G. E. Tupholme, An analogy between radially-loaded rubber bush mountings and axially-loaded bonded rubber blocks, Mater. Design 32(10) (2011) 5038-5042.
[12] K. Sedlaczek, S. Dronka, J. Rauh, Advanced modular modelling of rubber bushings for vehicle simulations, Vehicle Syst. Dyn. 49(5) (2011) 741-759.
[13] M. Cerit, E. Nart, K. Genel, Investigation into effect of rubber bushing on stress distribution and fatigue behaviour of anti-roll bar, Eng. Fail. Anal. 17(5) (2010) 1019-1027.
[14] https://www.researchgate.net/figure/Design-of-a-type-A-radial-shaft-seal_fig2_340443667
[15] T. J. Pence, K. Gou, On compressible versions of the incompressible neo-Hookean material, Math. Mech. solids 20(2) (2015) 157-182.
[16] R. S. Rivlin, K. N. Sawyers, Strain-energy function for elastomers, Trans. Soc. Rheol. 20 (1976) 54557.
[17] Y. Zhou, Z. Q. Huang, L. Tan, et al., Cone bit bearing seal failure analysis based on the finite element analysis, Eng. Fail. Anal. 45 (2014) 292-299.

International Journal of Innovative Research of Science, Engineering and Technology (IJIRSET)

Impact Factor 8.699

|www.ijirset.com |A Monthly, Peer Reviewed & Refereed Journal| e-ISSN: 2319-8753| p-ISSN: 2347-6710|

Volume 14, Issue 2, February 2025

|DOI: 10.15680/IJIRSET.2025.1402088|

[18] M. C. Chen, X. C. Ping,W. H. Liu, et al., A novel hybrid finite element analysis of two polygonal holes in an infinite elastic plate, Eng. Fract. Mech. 83 (2012) 26-39.
[19] C. O. Horgan, The remarkable Gent constitutive model for hyperelastic materials, Int. J. Nonlin. Mech. 68 (2014) 9-16.
[20] K. Patra, R. K. Sahu, A visco-hyperelastic approach to modelling rate-dependent large deformation of a dielectric acrylic elastomer, Int. J. Mech. Mater. Des. 11(1) (2015) 79-90.
[21] W. Kin, H. Chung, M. Cho, Anisotropic hyperelastic modeling for face-centered cubic and diamond cubic structures, Comput. Method. Appl. M. 291(1) (2015) 216-239.
[22] S. Kundurthi, P. Mythravaruni, P. Ravindran, Vulcanization and the mechanical response of rubber, Z. Angew. Math. Phys. 66(3) (2015) 1109-1123.
[23] M. R. Mansouri, H. Darijani, Constitutive modeling of isotropic hyperelastic materials in an exponential framework using an elf-contained approach, Int. J. Solids and Struct. 51(25-26) (2014) 4316-4326.
[24] R. Osterlof, H.Wentzel, L. Kari, An efficient method for obtaining the hyperelastic properties of filled elastomers in finite strain applications, Polym. Test. 41 (2014) 44-54.
[25] K. Patra, R. K. Sahu, A visco-hyperelastic approach to modelling rate-dependent large deformation of a dielectric acrylic elastomer, Int. J. Mech. Mater. Des. 11(1) (2015) 79-90
[26] D. S. Dogan, A. Demirer, Determination of characteristics of natural rubber/styrene-butadiene rubber-based elastomer material filled with mica powder and glass spheres, J. Elastom. Plast. 47 (2015) 306-319.
[27] R. Rashetnia, S. Mohammadi, Finite strain fracture analysis using the extended finite element method with new set of enrichment functions, Int. J. Numer. Meth. Eng. 102(6) (2015) 1316-1351.
[28] H. B. Yang, F. Z. Li, T. W. Chan, et al., A simulation study on the effect of spring-shaped
[29] Abaqus user's manual.

INTERNATIONAL STANDARD SERIAL NUMBER INDIA

INNO SPACE SJIF Scientific Journal Impact Factor

doi cross ref

निस्केयर NISCAIR

INTERNATIONAL JOURNAL OF INNOVATIVE RESEARCH

IN SCIENCE | ENGINEERING | TECHNOLOGY

9940 572 462 6381 907 438 ijirset@gmail.com

www.ijirset.com

Scan to save the contact details